EXPERIMENTAL STUDY ON VITRIFICATION OF CRYOPROTECTANTS USING THIN-FILM EVAPORATION OF NITROGEN

Henrique Roth Vidaletti[a*], Alisson Renan Stochero Da Silva[a*], Jacqueline Biancon Copetti[a], Mario Henrique Macagnan[a], Jeferson Dichi De Oliveira[b], Elaine Maria Cardoso[c], Leonardo Manetti[d]

[a]UNISINOS - University of Vale do Rio dos Sinos; Polytechnic School, 950, São Leopoldo - RS, Brazil
hvidaletti@yahoo.com.br, alissonstochero@hotmail.com, jcopetti@unisinos.br, mhmac@unisinos.br
[b]USP- University of São Paulo, Polytechnic School, SISEA - Renewable and Alternative Energy Systems Laboratory, São Paulo-SP, Brazil jef.diehl@usp.br
[c]UNESP - São Paulo State University, School of Engineering, São João da Boa Vista-SP, Brazil
elaine.cardoso@unesp.br
[d]IFMS - Federal Institute of Mato Grosso do Sul
leonardo.manetti@ifms.edu.br

ARTICLE INFO

***Keywords**: evaporation heat transfer, cell vitrification, liquid nitrogen, cryopreservation.*

Received: Jan 15, 2024
Reviewed: Feb 20, 2024
Accepted: Mar 01, 2024

ABSTRACT

Nitrogen thin film evaporation is a novel technique applied to cryopreservation, which aims to improve the preservation of biological samples at ultra-low temperatures. Cryopreservation is a critical process used in various fields, including biomedical research, regenerative medicine, and the storage of genetic materials. Traditional cryopreservation methods often suffer from sample damage caused by ice crystal formation and chemical toxicity associated with conventional cryoprotectants. This study developed an experimental apparatus comprising a vacuum chamber and two cryocauteries. The sample is stored in a polydimethylsiloxane-based composite reservoir between two copper plates with a nickel microporous outer surface. This system is suspended inside the chamber, and nitrogen jets promote evaporation. Chamber pressure and sample temperatures are recorded during the experiments. Tests were performed using dimethyl sulfoxide, glycerol and sucrose solutions in phosphate-buffered saline at different concentrations and volumes to evaluate vitrification and cooling rates. Effects of volume and concentration were evaluated, and it was found that vitrification success is directly related to the cryoprotective agent concentration used. In addition, no significant impact on the visual appearance of the samples related to vitrification regarding the sample geometry was observed. The copper foam porous surface resulted in the highest cooling rate, which is associated with the properties of the foam, such as its high thermal conductivity.

NOMENCLATURE

a	Cell diameter, mm
d_f	Fiber diameter, mm
d_p	Pore diameter, mm
CPA	Cryoprotective agents
DMSO	Dimethyl sulfoxide
LN2	Liquid nitrogen
PBS	Phosphate-buffered saline
PDMS	Polydimethylsiloxane

Greek symbols

ρ	Density, kg/m^3
ε	Porosity, %

1. INTRODUCTION

Cryopreservation has evolved as a technology for medical applications such as cell therapy, tissue engineering, assisted reproduction and gene therapy. This process allows preserving biological material at low temperatures, generally between -80 and -196 ºC,

* Corresponding author: Jacqueline Biancon Copetti. UNISINOS - University of Vale do Rio dos Sinos; Polytechnic School, 950, São Leopoldo - RS, Brazil. jcopetti@unisinos.br

suppressing biological aging and maintaining viability. Freezing and storage are done through contact of the material with cryogenic fluid and cryoprotective agents, minimizing osmotic damage and preventing the formation of intra and extracellular ice crystals, thus reducing cryo damage.

The viability of living systems mainly depends on the presence of water. Removing water from tissues, cells or biomolecules through freezing can lead to cellular damage. This removal can cause osmotic stress or conformal changes that affect the structure and function of cells and biomolecules. Furthermore, ice formation can cause mechanical stresses on biological materials. One way to preserve the life of these cells during freezing processes is the development of protocols and formulations focused on protecting these materials (Wolkers et al., 2021).

In conventional protocols or slow freezing with gradual temperature reduction, the sample is placed in straws or cryotubes, kept in a deep freezer in the first step, and then shifted to liquid nitrogen banks. The low cooling rates (10-100 °C/min) can result in crystallization problems and dehydration.

An alternative to obtain higher cooling rates is vitrification, in which the sample passes directly from the liquid state to the vitreous and amorphous state, without the formation of ice crystals, when exposed to extremely low temperatures and high cooling rates. However, vitrification requires higher concentrations of CPA to protect cells from damage caused by dehydration. Therefore, new vitrification techniques are being tested and investigated, seeking to increase the cooling rate, using smaller volumes of material and lower concentrations of CPA, in order to achieve adequate conditions and reduce the toxicity and damage caused to cells by crystals of ice during the process (Li et al., 2019).

There are methods such as Cryoloop (Lane et al., 1999), Open Pulled Straw (Vajta et al., 1998), Droplet Vitrification and Electron Microscopy Grids (Martino et al., 1996), which can achieve complete or partial vitrification of small samples, in rates about 20,000 ºC/min, but require the use of high concentrations of CPA. A technique based on the evaporation of a thin film of liquid nitrogen over a microporous surface has been proposed as an approach to vitrification. Su et al. (2018) obtained significant results using samples with different concentrations of DMSO and volume of 3μL, reaching high freezing rates.

Heat transfer in thin film evaporation can be analyzed in relation to different regions and their respective associated thermal resistances (Plawsky et al., 2014). These regions include the adsorbed or non-evaporating thin film region, the transition region, where the attractive forces of the liquid on the solid are weak, and the liquid-vapor interface has measurable curvature, and the meniscus or bulk fluid region, where the curvature of the liquid-vapor interface becomes almost constant, acting as a liquid reservoir for the transition region. Associated thermal resistances include conduction through the solid substrate, conduction through the liquid (which is a linear function of film thickness), and resistance to heat transfer at the liquid-vapor interface, which depends on intermolecular forces, film thickness, liquid-vapor curvature, and mass vapor state.

In order to improve heat transfer during phase change, it is important to maximize the region where the overall thermal resistance is reduced and to minimize the hydrodynamic resistances related to the liquid flow into and vapor flow out of this region. Surface modification techniques, such as microstructured or microporous surfaces, have been employed to control the transport processes. Surface morphology can alter interactions between solid, liquid and vapor, maximizing the region where phase change is most active. In addition, the microstructured surface increases the solid-liquid contact area, which favors capillary absorption (Liu et al., 2011) and nucleation sites, improving heat transfer during phase change (Maroo and Chung, 2013). Additionally, the wettability can be modified, affecting fluid flow processes.

The current work presents the research results that have been carried out using thin film evaporation of LN2 for sample vitrification using a surface coated with metal foam. The aim is to analyze the cooling process considering CPA samples, usually used with semen (future application of this research), in different concentrations and volumes, as well as foam coatings, characterizing the vitrification conditions and freezing rates.

2. EXPERIMENTAL PROCEDURE

The experimental study of vitrification by thin-film evaporation was carried out in an experimental apparatus developed, as shown in Figure 1. It consists of an acrylic chamber (a) and two cryocautery (Nitrospray, 500 ml) containing nitrogen (b). The sample is stored in a PDMS device between 2 copper plates coated with metal foam (c and d). This system is suspended inside the chamber, and two nitrogen jets (mass flow of 1.2 ± 0.1 g/s, determined by experimental tests) are applied on both sides of the porous surface, promoting evaporation. The pressure inside the chamber and temperatures in the sample are recorded during the experiments.

The temperatures and pressure recording is performed using a data logger (Novus) connected to a computer, with an acquisition time of 50 ms. A pressure transducer (Keller - PA33X/80794) performs the internal pressure measurement, and the temperature measurements are performed using two T-type thermocouples (measurement uncertainty of ±1°C) positioned in the sample and inside the chamber. Two vacuum pumps (EOS) help to

establish the internal condition to activate the cryocautery, promote film evaporation, and remove the nitrogen vapor from the chamber. Images and videos of the evaporation process were recorded with a high-speed camera (Motion Pro Y4).

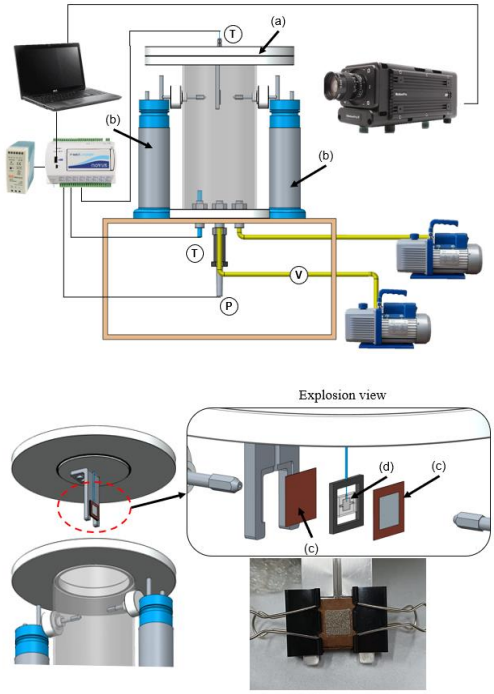

Figure 1. Experimental apparatus for tests with LN2 thin-film: a.chamber; b. cryocautery; c. surfaces with metal foam; d. PDMS device with sample

The temperatures and pressure recording is performed using a data logger (Novus) connected to a computer, with an acquisition time of 50 ms. A pressure transducer (Keller - PA33X/80794) performs the internal pressure measurement, and the temperature measurements are performed using two T-type thermocouples (measurement uncertainty of ±1°C) positioned in the sample and inside the chamber. Two vacuum pumps (EOS) help to establish the internal condition to activate the cryocautery, promote film evaporation, and remove the nitrogen vapor from the chamber. Images and videos of the evaporation process were recorded with a high-speed camera (Motion Pro Y4).

2.1 PDMS device for samples

The device containing the sample was manufactured in polydimethylsiloxane-based composite (PDMS) due to its biocompatibility with reproductive cells; it also has elasticity, resistance, transparency, and easy prototyping. In this way, the sample is not in direct contact with the LN2, avoiding contamination during freezing and thawing.

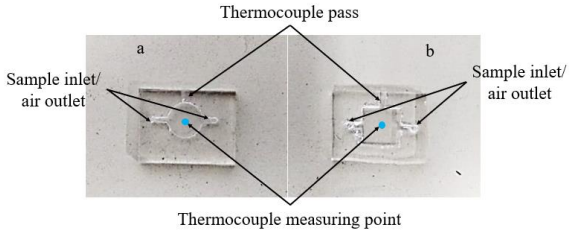

Figure 2. Different PDMS devices analyzed in the current study: a) 30 μL; b) 38 μL.

2.2 Metal Foam Characteristics

Different metal foams, nickel and copper, were analyzed. The metal foams with 1 mm in thickness were welded on the copper plates (20 × 20 ×1 mm^3), and the characterization was performed by Manetti et al. (2020), as shown in Table 1. Different techniques were employed to measure their porosity (ε), density (ρ), cell diameter (a), and pore and fiber diameter (d_p and d_f), respectively.

Table 1. Main characteristics of nickel and copper metal foams.

Foam	SEM image	ρ_{foam} (kg/m³)	ε (%)	a (mm)	d_p (mm)	d_f (mm)
Ni	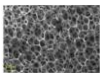	138 ± 14.12	98.4 ± 0.15	0.46 ± 0.10	0.25 ± 0.09	0.07 ± 0.02
Cu	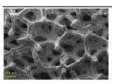	908 ± 28.63	90.0 ± 0.32	1.08 ± 0.24	0.52 ± 0.22	0.09 ± 0.04

2.3 Samples and tests

Tests were carried out using CPA samples of DMSO, glycerol and sucrose in PBS (Phosphate-buffered saline) at different concentrations and volumes to evaluate the cooling rates and the sample vitrification through visual analysis. With the data collected from the tests, the cooling rates were calculated, corresponding to the ratio of temperature variation over a given time, as shown in Equation 1.

$$\frac{\Delta T}{\Delta t} = \frac{T_{Final} - T_{initial}}{t_{final} - t_{initial}} \quad (1)$$

The cooling intervals were established considering the thermodynamically unstable region between the homogeneous nucleation temperature (in our study, it corresponds to 12 °C) and the glass-transition temperature (- 137 °C) as proposed by Akiyama et al. (2019), where they describe a method

for the CPA-free cell cryopreservation of mammalian cells by ultrarapid cooling. Immediately after assembling the samples inside the chamber, the tests followed the vacuum procedure of around 15 kPa. Upon reaching this pressure, the cryocautery was manually activated, reducing the temperature of the samples. The cryocautery and vacuum were activated upon reaching the minimum stable temperature, the sample set was disassembled, and the sample image was recorded.

2.4 Effect of CPA and concentration

Tests were conducted to investigate the relationship between CPA concentration, cooling rates, and the vitrification condition. The samples were cooled using three different cryoprotectants (DMSO, glycerol and sucrose) in two different concentrations (50% and 30%). During the process, the temperature of the samples decreased from approximately 20 °C to approximately -180 °C.

Figure 3 presents the cooling rate results for DMSO, and Figure 4 presents the cooling rate results for glycerol with different concentrations during evaporation over the nickel foam. One may observe that for glycerol, Figure 4, the concentration did not significantly impact the cooling rate behavior. The greatest discrepancy between the curves occurred for a temperature range from 0 °C to -50 °C, resulting in a cooling rate difference of approximately 93 °C/min. However, by analyzing the visual aspect of the samples, it was found that the sample with the highest concentration of CPA (50%) resulted in vitrification, while the sample with the lowest concentration had ice-crystal growth.

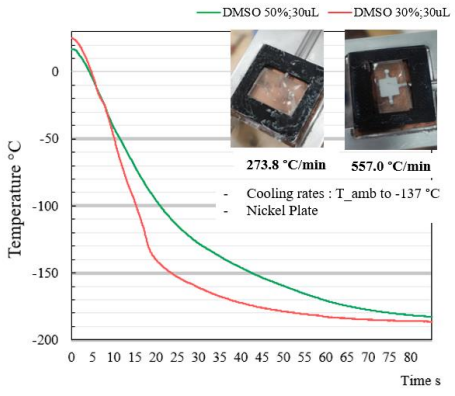

Figure 3. Temperature variation and cooling rates for 30 µL of DMSO at 50% and 30%.

For DMSO (Figure 3), the lowest the CPA concentration, the highest the cooling rate. As previously observed, vitrification occurred for the highest concentration, and crystallization occurred for the lowest cryoprotectant concentration.

Therefore, vitrification success is directly related to the CPA concentration used for these specific cases. Furthermore, there is no evidence of a direct relationship between cooling rates and sample vitrification. This finding can be seen in Figure 5, in which all CPAs analyzed in the current work were shown. The highest cooling rates were found for those samples with low cryoprotectant concentrations (Figure 6). On the other hand, complete vitrification was observed in samples with high concentrations (Figure 5).

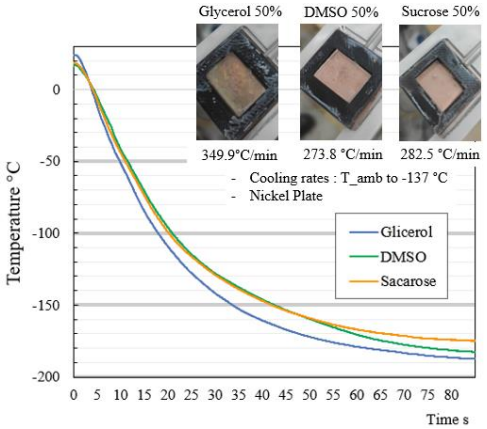

Figure 5. Temperature variations and cooling rate for 30 µL of Glycerol, DMSO and Sucrose for concentrations of 50%.

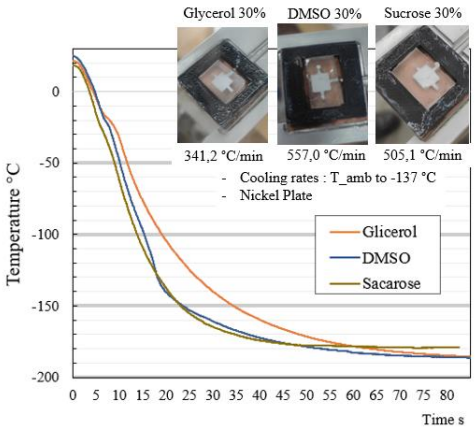

Figure 6. Temperature variations and cooling rate for 30 µL of Glycerol, DMSO and Sucrose for concentrations of 30%.

2.5 Effect of PDMS geometry and volume

The influence of sample geometry, square of 30 µL and circular of 38 µL, on the cooling rate was also evaluated. Although some results showed differences in cooling rates, the expected result — for a lower volume, a higher cooling rate would be achieved — was not verified; such behavior may be due to the small difference in the volume of the two devices.

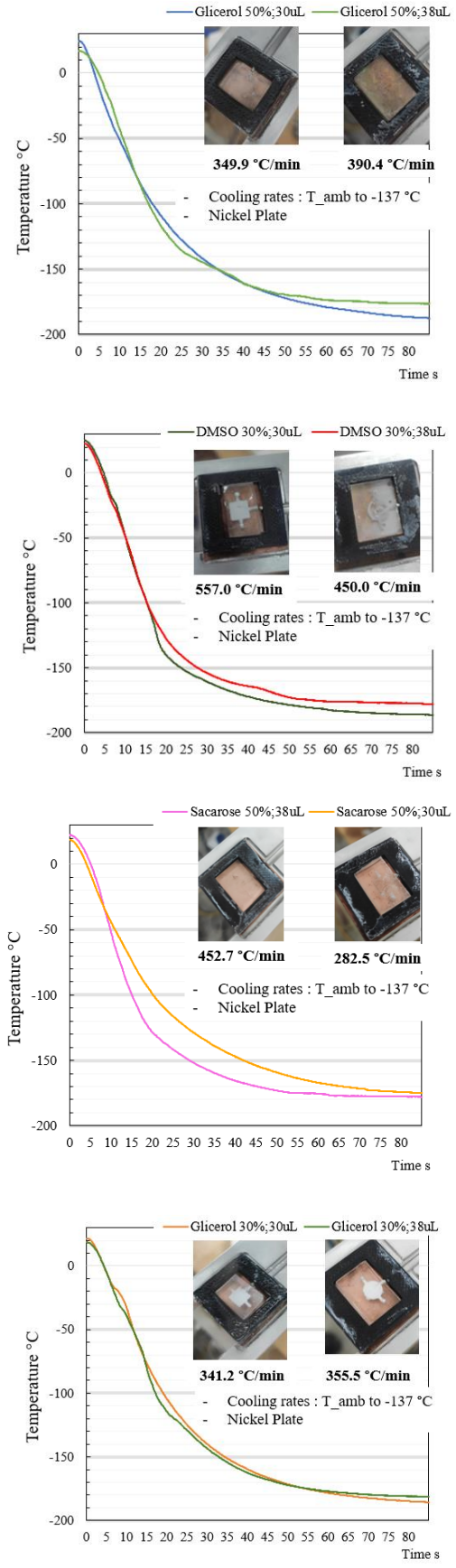

Figure 7. Comparative cooling rates and visual appearance for different sample device geometries and volumes.

2.6 Effect of the microporous surface on the process

Figure 8 shows the cooling rates for the DMSO (50%) in order to compare the cooling behavior for porous surfaces (nickel and copper foam plates) with that for plain surfaces (smooth copper plate). Significant differences in cooling rates were observed; the porous surface with copper foam resulted in the highest cooling rate, which is associated with the properties of the foam (Table 1), such as the highest thermal conductivity.

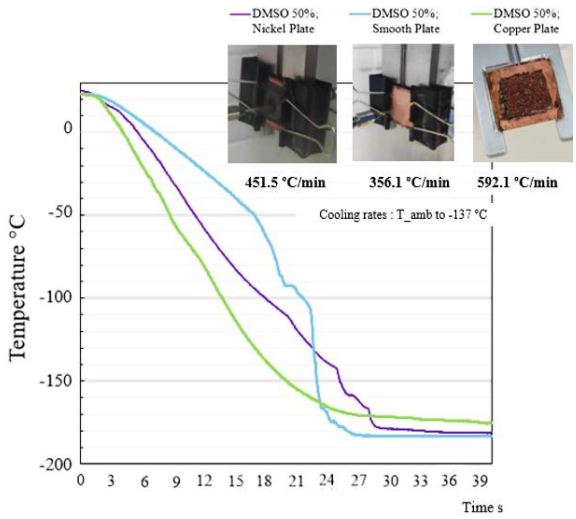

Figure 8. Influence of the porous surface on the cooling rate performance.

For copper foam, a more pronounced temperature drop was observed compared to the plain surface (cooling rate of 592.1 °C/min from room temperature up to -137 °C), promoted by the microporous structure responsible for promoting increased heat transfer to the PDMS reservoir. A similar behavior was found for nickel foam.

3. CONCLUSION

The current study presented an approach using nitrogen thin-film evaporation for cryopreservation, aiming to enhance the preservation of biological samples at ultra-low temperatures. The conventional cryopreservation methods often encounter challenges such as sample damage due to ice crystal formation and chemical toxicity from cryoprotectants. Tests were conducted using different concentrations and volumes of DMSO, glycerol, and sucrose solutions in PBS to evaluate vitrification and cooling rates. A direct relationship was found between the concentration of cryoprotective agents (CPA) used and the success of vitrification. Additionally, the sample geometry does not seem significantly to affect the vitrification process. The copper foam porous

surface demonstrated the highest cooling rate among the tested surfaces. This can be attributed to the favorable properties of the foam, such as its high thermal conductivity, which facilitated efficient heat transfer and accelerated the cooling process.

These findings highlight the potential of nitrogen thin-film evaporation as a promising technique for cryopreservation. The use of copper foam, with its enhanced cooling capabilities, further contributed to the success of the cryopreservation process. This study provides valuable insights into applying nitrogen thin-film evaporation in cryopreservation and demonstrates its potential for various fields, including biomedical research, regenerative medicine, and genetic material storage. Further research and optimization are necessary to explore the full potential of this technique and its broader implications in practical cryopreservation applications.

4. ACKNOWLEDGEMENTS

The authors gratefully acknowledge the financial support of MCT/CNPq (Brazilian National Council of Research) under contract 403825/2021-0. The authors also acknowledge the grants provided by the Capes and CNPq agencies and the company HemoCord-Umbilical Cord Blood Bank for technical and material support. E.M.Cardoso would like to thank UNESP for the financial support provided by PPGEM – UNESP/FEIS, CNPq (309848/2020-2 and 305040/2023-5) and FAPESP (2013/15431-7 and 2019/02566-8).

5. REFERENCES

Akiyama, Y., Shinose, M., Watanabe, H., Yamada, S., Kanda, Y. 2019. Cryoprotectant-free cryopreservation of mammalian cells by superflash freezing. Proceedings of the National Academy of Sciences, 116, 7738–7743.

Lane, M., Schoolcraft, W.B., Gardner, D.K. 1999. Vitrification of mouse and human blastocysts using a novel cryoloop container-less technique. Fertility and Sterility, 72.

Li, Y., Memon, K., Zheng, Y., Cheng, Y., Mbogba, M. K., Wang, P., ... & Zhao, G. 2019. Microencapsulation facilitates low-cryoprotectant vitrification of human umbilical vein endothelial cells. ACS Biomater Sci Eng, *5*(10), 5273-5283.

Liu, W., Li, Y., Cai, Y., Sekulic, D.P. 2011. Capillary Rise of Liquids over a Microstructured Solid Surface. Langmuir, 27, 14260–14266.

Manetti, L.L, Ribatski, G., de Souza, R.R., Cardoso, E.M. 2020. Pool boiling heat transfer of HFE-7100 on metal foams. Exper. Therm. Fluid Sci., 113.

Maroo S.C., Chung, J.N. 2013. A Possible Role of Nanostructured Ridges on Boiling Heat Transfer Enhancement. Journal of Heat Transfer, 041501.

Martino A., Songsasen, N., Leibo, S.P. 1996. Development into blastocysts of bovine oocytes cryopreserved by ultra-rapid cooling. Biology of Reproduction, 54, 1059-1069.

Plawsky, J.L.; Fedorov, A.G.; Garimella, S.V.; Ma, H.B.; Maroo, S.C.; Chen, L.; Nam, Y. 2014. Nano and microstructures for thin-film evaporation – A review. Nanoscale and Microscale Thermophysical Engineering, 18, 251–269.

Su, F., Zhao, N., Deng, Y., and Ma, H. 2018. An Ultrafast Vitrification Method for Cell Cryopreservation. ASME. J. Heat Transfer, 140, 012001.

Vajta, G., Holm, P., Kuwayama, M., Booth, P.J., Jacobsen, H., Greve, T., Callesen, H. 1998. Open pulled straw (OPS) vitrification: A new way to reduce cryoinjuries of bovine ova and embryos. Molecular Reproduction and Development, 51, 53-58.

Wolkers F.W.; Oldenhof, H. 2021. Cryopreservation and Freeze-Drying Protocols. Springer Protocols. Fourth Edition.